

# Unilateral Fixtures for Sheet Metal Parts with Holes\*

K. “Gopal” Gopalakrishnan, Ken Goldberg, Gary M. Bone, Matthew Zaluzec, Rama Koganti, Patricia Deneszczuk

**Abstract**—Existing fixtures for holding sheet metal parts are generally bulky, part-specific, and designed by human trial-and-error. In this paper, we propose *unilateral fixtures*, a new class of fixtures that addresses these limitations using modular fixturing elements that lie almost completely on one side of the part, maximizing access on the other side for welding, assembly, or inspection. The primary holding elements are cylindrical jaws with conical grooves that expand between pairs of part hole corners; each grooved jaw provides the equivalent of four point contacts and facilitates part alignment during loading.

We present a two-phase algorithm for designing unilateral fixtures. The first phase assumes the part is rigid and uses 2D and 3D kinematic analysis of form-closure to identify all pairs of candidate jaw locations. For this analysis we propose and prove three new grasp properties for 2D and 3D grips at concave vertices, and a new quality metric based on the sensitivity of part orientation to infinitesimal relaxation of jaw position. The first phase also sets bounds on jaw cone angles. The second phase addresses part deformation with a Finite Element Method (FEM) analysis that arranges secondary contacts at part edges and interior surfaces.

For a given sheet-metal part, given as a 2D surface embedded in 3D with  $n$  concavities and  $m$  mesh nodes, the kinematic algorithm takes  $O(n^2)$  time to compute a list of all unilateral fixtures ranked by quality, or a report that none exist for that part. The FEM deformation analysis arranges  $r$  secondary contacts considering  $m$  part elements in  $O(m^3r)$ . We have implemented both phases of the algorithm and report alignment data from experiments with two physical parts.

**Index Terms** — Assembly, Fixturing, Form-Closure, Grasping, Modular Fixturing, Sheet Metal, Welding, Workholding.

## I. INTRODUCTION

SHEET metal parts are created by stamping and bending planar sheets. To assemble industrial parts such as automotive bodies and large appliances, such sheet metal panels need to be accurately located and held in place by fixtures to permit assembly, welding, or inspection. Existing fixturing methods are usually: bulky (limiting access to the part), dedicated to each part (requiring a large investment in materials), and designed by human intuition (introducing delays and suboptimal designs).

---

Manuscript received December 15, 2002. This work is supported in part by the Ford Motor Company and NSF Award DMI-0010069.

K. Gopalakrishnan and K. Goldberg are with the University of California at Berkeley, Berkeley, CA 94720 USA (phone: 510-643-2030; fax: 510-643-2030; e-mail: gopal@ieor.berkeley.edu; goldberg@ieor.berkeley.edu).

G. M. Bone is with McMaster University, Hamilton, Ontario, Canada L8S 4L7 (email: gary@mcmaster.ca).

M. Zaluzec, R. Koganti and P. Deneszczuk are with the Ford Motor Company, Dearborn, MI 48121 USA (email: mzaluzec@ford.com; rkoganti@ford.com; pdeneszc@ford.com).

We propose *unilateral fixtures*, a new class of fixtures that addresses these limitations using modular fixturing elements that lie almost completely on one side of the part, maximizing access on the other side. The primary holding elements are cylindrical jaws with conical grooves that expand between pairs of part hole corners; each grooved jaw provides the equivalent of four point contacts and facilitates part alignment during loading. We define and give an algorithm that analyzes the sheet-metal geometry and automatically designs unilateral fixtures.

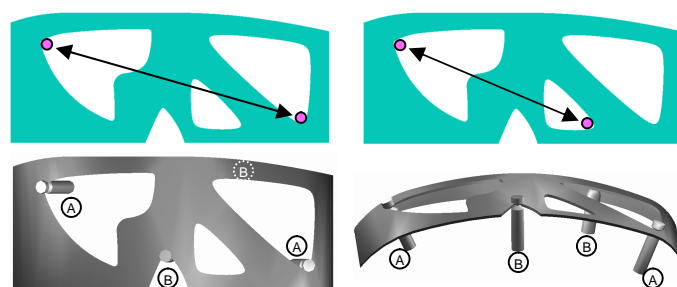


Fig. 1. 2D analysis and 3D unilateral fixture (2 views). Primary jaws (A) hold the 3D sheet metal part in form-closure and secondary jaws (B) minimize deformation.

We present a two-phase design procedure for unilateral fixtures. The first phase is a geometric algorithm that assumes the part is rigid and locates one pair of primary jaws to immobilize the rigid part. This phase is purely kinematic in its analysis. The second phase adds additional secondary jaws using a heuristic Finite Element Method (FEM) procedure to reduce deformation to within specified tolerances.

For the first phase, we locate pairs of concavities of the part where jaws can be placed. For every pair of concavities, we apply a set of sufficient conditions to test the part for immobility. We show that the 3D sheet metal part is fixtured by jaws at these concavities if 2D parts that are projections of the 3D sheet metal part on to 2 orthogonal planes containing both concavities are fixtured by the projections of the jaws and if the conical grooves of the jaws prevent rotation about an axis through both concavities.

To check for fixturing in 2D, we consider the distance between the 2D jaws. We show that when the jaws are at different concavities, the distance between the jaws needs to be at an extremum in order to fixture the part. We have presented this part of the work earlier in [8]. We also derive a 2D quality metric based on the maximum possible change in the part's orientation when jaw position is relaxed infinitesimally. We then extend this quality metric to 3D as a measure of the largest component of the change in the 3D sheet metal part's orientation when the distance between the jaws is relaxed infinitesimally.

We note that one pair of primary contacts suffice to immobilize the rigid 3D part as each jaw contacts the part at 4 points: 2 points in the cross-section, and for each of these, on either surface of the part. Thus 2 jaws can provide the equivalent of 8 point contacts; while in general, 7 are sufficient to immobilize a 3D part. These fixtures are an example of minimalist robotics, or RISC, as presented in [5].

The fixtures described in this paper also possess a self-aligning nature, i.e. they align the part into the correct orientation as the part is loaded on to the fixture. We perform repeated tests on 2 example parts to check the distributions of errors in orientations when loaded on numerous fixtures.

## II. RELATED WORK

Grasping and fixturing both involve holding a part in a way that limits its mobility. Bicchi and Kumar [2] and Mason [12] provide concise surveys of research on robot grasping. Fixturing may further involve a reduced set of components such as clamps or locators to create modular fixtures. More recent work also covers the aspect of fixturing deformable parts.

Grasps can be classified as force or form-closure. Form-closure occurs when any neighboring configuration of the part results in collision with an obstacle. Force-closure occurs if any external wrench can be resisted by applying suitable forces at the contacts [12, 21]. Gripper contacts can be modeled as frictional points, frictionless points or soft contacts [24]. [19] and [26] prove that 4 and 7 frictionless point contacts are necessary to establish form-closure in the plane and in 3D respectively and [14] and [11] proved that 4 and 7 point contacts suffice.

Rimon and Burdick [Rimon96, 98] were the first to identify and introduce the notion of second order force-closure. Immobility is defined to occur if any trajectory results in the decrease of distance between the part and at least one obstacle it is in contact with. First and Second orders of immobility arise due to the truncation of the Taylor expansions of the distances at the first and second order terms respectively. [20] shows that generic planar parts can be immobilized (second-order) with three frictionless contacts if they are placed with infinite precision. Ponce et al [17] give an algorithm to compute such configurations.

Rimon and Blake [22] give a method to find *caging grasps*, configurations of jaws that constrain parts in a bounded region of C-space such that actuating the gripper results in a unique final configuration. They consider the opening parameter of the jaws as a function of their positions and use stratified Morse theory to find caging grasps. In this paper, we look at the distance between the jaws and use the fact that they are at a strict extremum to show that the part is immobilized.

Plut and Bone [15, 16] proposed inside-out and outside-in grips using two or more frictionless point contacts at linear or curved part edges. They show how to find such grips where the distance between contacts is at an extremum. They achieve form-closure in 3D using horizontal V-shaped circumferential grooves (VCGs). Our unilateral model minimizes fixture profile on one part exterior and generalizes their analysis with

an exact test for 3D form-closure, a new quality metric, and a method for locating secondary contacts based on FEM.

In fixturing, Hurtado and Melkote [9] study how a fixture's conformability and stability vary with design parameters such as number and positions of contacts and geometric properties of the fixture elements. They develop two metrics based on global and local conformability (based on similarity of shape between the part and the circumscribing polyhedron fitting the contacts). By minimizing the net complementary energy of the fixture and part system, the reactionary forces were evaluated at the contacts and used to observe trends of conformability and stability as the design parameters varied. Wang [29] examines the errors in machined features in relation to the errors in locator position and locator surface geometric errors. The relation is expressed using a critical configuration matrix for the part. Wang suggests an optimal locator configuration based on error sensitivity of multiple features machined on the part. Wang and Liu [30] examine fixture design based on part curvature at the points of contact. They call their model a full-kinematic model and it helps design fixtures with considerations of location precision. This is achieved since they analyze part geometry in greater detail (including part curvature). Xiong et al [31] develop a statistical model for analysis of geometric variations in assemblies. They model the stacking of incremental errors in each assembly station, and based on locator errors and geometric errors of individual parts, determine the error in position or orientation of the feature being analyzed. The predicted errors are used to study assembly methods and sequences to choose an optimal assembly process.

An efficient geometric algorithm to compute all placements of four frictionless point contacts on a polygonal part that ensure form-closure is described by van der Stappen et al [27]. Given a set of four edges, they show how to compute critical contact placements in constant time. The time complexity of their algorithm is bounded by the number of such sets. For the specialized case of v-grips, their algorithm runs in an expected time of  $O(n^2 \log n)$  for  $n$  vertices.

A lot of recent work on fixturing deformable and sheet-metal parts is based on the work of Menassa and De Vries [13] where they determine the positions of the primary datum (the datum points needed to locate the part in the correct plane) for 3-2-1 fixturing to minimize deformation. They use a finite element model of the part to model the deformation, and determine fixture locations by optimizing an objective that is a function of the deformations at the nodes. Their work is extended by [18] and [4]. [18] designs a fixture for a sheet metal part by using an objective function that is a weighted sum of the norm of the deformation and the number of fixtures in the objective function. They use a remeshing algorithm, but do not address properties specific to sheet metal parts such as buckling. Cai et al describe an N-2-1 fixturing principle in [4]. This is used instead of the conventional 3-2-1 principle to reduce deformation of sheet-metal parts. They use N ( $\geq 3$ ) locators for the primary datum, (i.e. they use N datum points to locate the sheet metal part in the correct plane) in their fixtures. They model the sheet metal parts using finite

elements with quadratic interpolation, constraining nodes in contact with the primary datum to only in-plane motion. For a known force, linear static models are used to predict deformation. To make their algorithm faster, instead of remeshing the part for different locator positions, they express the constrained displacement at the locator by using a linear interpolation of displacement at the adjacent nodes. Fixture elements are placed such that compressive forces that cause buckling do not occur. In contrast, our two phase approach is a hybrid of geometric and FEM methods.

[28] and [6] study using discretized domains of fixture element locations to create fixtures. [28] describes an algorithm to obtain an optimal fixture for a domain of discrete contacts with 6 locators and one clamp. The optimality is obtained by considering localization accuracy and force balance at the contacts. [6] proposes a method for fixture design for curved workpieces by discretizing the part's surface to obtain contact locations. They start with a random set of contacts and randomly iterate contact locations till form-closure is achieved. The number of iterations is reduced by eliminating sets of contacts based on a facet that divides the domain of contacts into 2 parts based on the property that the contact wrenches need to positively span the wrench space. Only half-space defined by the facet is considered. Li et al [10] describe a procedure to design fixtures for two sheet metal parts that are to be welded to produce a good fit along the seam to be welded. The fixtures are designed using a finite element model to determine either an optimal fixture or a robust fixture.

For modular fixtures, Brost and Goldberg [3] present the first complete synthesizing algorithm that guarantees to find a fixture, consisting of 3 locators and 1 clamp if one exists. They enumerate all such fixtures by choosing candidate fixture element positions that are at a distance permitted by the edges of the part the elements are in contact with. Rong and Li [23] present an interactive Rapid Fixture Design System (RFDS) that allows a designer to make use of several databases of fixture components, location method, etc. and automates the generation of a modular fixture subject to the specifications of the user regarding positions and orientations of the components. [25] considers the fixturing of a sheet metal workpiece using clamps and locators fixed on a base-plate with t-slots. The height of the fixture elements are variable, and are adjusted to fit the shape of the part. Determining the positions of the locators and clamps is formulated as a non-linear programming problem in terms of the part deformation.

The unilateral fixturing approach is inspired by Toyota's "Global Body Line" auto assembly system [7]. This system fixtures different auto models using a reduced set of hardware that includes an "inside locator jig". We have been unable to find any details on analytical models for the GBL system.

### III. PROBLEM STATEMENT

The input is a model of a sheet metal part sheet metal part: a contiguous connected 2D surface with holes whose thickness is assumed to be small compared to the dimensions of the features on the part. It is defined by a CAD model that consists

of a list of its edges: both external and internal (holes) in terms of spline curves. For each edge, the side of the edge on which the part lies is also specified. A FEM mesh discretizing the part as a surface embedded in 3D is also specified. This is a triangular or quadrilateral mesh (but other meshes can be used in general). The part's thickness and material properties are also specified. Primary jaws consist of 2 coaxial frustums of cones joined at their narrow ends which have equal radii (called the radius of the jaw). Secondary jaws may either be of the same shape as primary jaws, or may be point contacts supporting the interior of the part (away from edges). All jaws are assumed to be rigid and all contacts are assumed to be frictionless. The part is subjected to a set of known external wrenches specified as a list describing each wrench vector and the node of the part's mesh where it is applied. For each node, the direction of the part's interior, i.e. the direction in which the unilateral fixture may lie, is specified. A tolerance  $\delta$  is specified. This is the maximum deformation (i.e. magnitude of displacement from original position) of any point on the part as a result of the applied wrenches.

**Input:** CAD model of part with FEM mesh (as specified above), Young's modulus and Poisson's ratio of the part, jaw radii, list of applied wrenches, and allowed tolerance  $\delta$ .

**Output:** A list of unilateral fixtures that specify positions and orientations of each jaw within the given tolerances and bounds on the cone angles of each primary jaw, or a report that no solution exists.

We note here that we present an algorithm only to design the fixture itself and not design a loading mechanism for the fixture.

To solve this problem we first establish some preliminary results regarding fixturing 2D parts with 2 jaws in section IV. These results will then be used in section V where we design the location and shape of the first 2 jaws of the 3D fixture which we refer to as the primary jaws. A quality metric to evaluate any given pair of primary jaws is also presented in section V. This is done based on part kinematics only. After the kinematic analysis phase, we move on to the second phase dealing with application of FEM deformation models to each pair of primary jaws that we compute to solve the problem. This is discussed in section VI. The entire algorithm is presented in section VII.

## IV. KINEMATIC ANALYSIS: 2D V-GRIPS

### A. Problem Definition

In order to establish fast sufficient conditions for immobility in the kinematic analysis phase of our design procedure for 3D unilateral fixtures, we need to make use of kinematic results on immobility of 2D parts presented in this section. We give necessary and sufficient conditions for fixturing a 2D part with 2 jaws. These conditions will be repeatedly called with projections of the 3D sheet metal part on to pairs of orthogonal planes as 2D parts.

We begin by defining **v-grips** in the plane. Given a planar projection of the part, we want to find and rank all available v-grips. We assume that the projection of the part onto the

horizontal plane is rigid and can be defined by a polygonal boundary and polygonal holes. All contacts are frictionless. We initially assume both jaws have zero radii.

Let  $v_a$  and  $v_b$  be two concave vertices. The unordered pair  $\langle v_a, v_b \rangle$  is an expanding or contracting  $v$ -grip if jaws placed at these vertices will provide frictionless form-closure of the part. A  $v$ -grip is expanding if the jaws move away from each other and contracting if the jaws move towards each other to acquire the part.

**Input:** Vertices of polygons representing part boundary and holes, in counter-clockwise order, and jaw radius.

**Output:** A list (possibly empty) of all  $v$ -grips sorted by quality measure.

### B. Test for Form-closure

The key to our algorithm is a constant-time test for form-closure. We consider a pair of concave vertices  $\langle v_a, v_b \rangle$ . Let  $v_{x-1}$  and  $v_{x+1}$  be the vertices adjacent to  $v_x$ . Let  $\mathbf{u}_{x-1}$  be the unit vector from  $v_x$  to  $v_{x-1}$ , and  $\mathbf{u}_{x+1}$  the unit vector from  $v_x$  to  $v_{x+1}$ . Let  $\mathbf{u}_{xy}$  be the unit vector from  $v_x$  to  $v_y$ .

We construct normals at  $v_a$ , to both edges bordering  $v_a$ . This splits the plane into 4 regions (see figure 2). We number these I to IV. We do a similar construction with  $v_b$ .

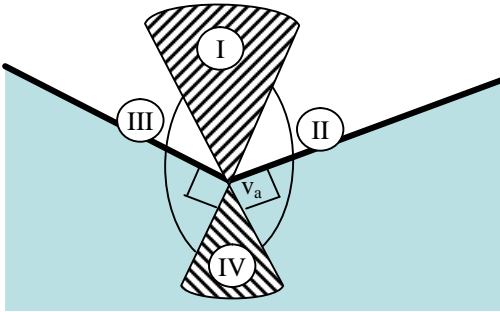


Fig. 2. Two normals at a concave vertex partition the plane into 4 regions that define  $v$ -grips.

**Theorem 1:**  $\langle v_a, v_b \rangle$  is an *expanding*  $v$ -grip if and only if  $v_a$  lies strictly in region I of vertex  $v_b$ , and  $v_b$  lies strictly in region I of vertex  $v_a$ .

**Theorem 2:**  $\langle v_a, v_b \rangle$  is a *contracting*  $v$ -grip if and only if either:

- (1)  $v_a$  lies in region IV of vertex  $v_b$ , and  $v_b$  lies in region IV of vertex  $v_a$ , at least one of them strictly, (or)
- (2)  $\mathbf{u}_x \cdot \mathbf{u}_y = -1$  and  $\mathbf{u}_x \cdot \mathbf{u}_{ab} = \mathbf{u}_y \cdot \mathbf{u}_{ab} = 0$  for at least one set of values of  $(x, y) = (a \pm 1, b \pm 1)$ , and the jaws approach from outside the region between the parallel lines (see figure 3).

### C. Proof of Theorem 1

Let  $P$  represent part perimeter parameterized by arclength  $s$ . Let  $s_a$  and  $s_b$  represent the positions of the jaws on  $P$ . Following [1] and [22], we express the distance between the jaws as  $\mathbf{s} : P \times P \rightarrow \mathfrak{R}$ , a function of  $(s_a, s_b)$ . The  $\sigma(s_a, s_b)$  surface is positive except when it touches the plane along the diagonal  $s_a = s_b$  (where it is 0), as these points represent coincident jaws. The  $s_a - s_b$  plane can be partitioned into rectangles whose sides are equal in length to the sides of the polygon. In each of these regions, the distance function is defined by a quadratic expression.

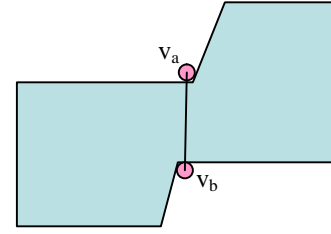


Fig. 3. Typical example of  $v$ -grips where the second condition in Theorem 2 holds.

To prove Theorem 1, we prove that the following 4 statements are equivalent:

A:  $v_a$  and  $v_b$  are concave and they each lie in the other's region I.

B:  $\sigma(s_a, v_b)$  is a strict local maximum at  $s_a = v_a$ , and  $\sigma(v_a, s_b)$  is a strict local maximum at  $s_b = v_b$ .

C:  $\sigma(s_a, s_b)$  is a strict local maximum at  $s_a = v_a$  and  $s_b = v_b$ .

D:  $\langle v_a, v_b \rangle$  is an expanding  $v$ -grip for the part.

$B \Leftrightarrow A$ : This is clearly seen since the shortest distance from a point to a line is along the normal to the line (figure 4).

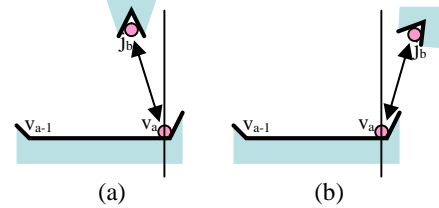


Fig. 4.  $j_b v_a$  is a strict local maximum (a) or a local minimum (b) for  $s_a$  in  $v_{a-1} v_a$ .

$C \Rightarrow B$  follows from the definitions.

$B \Rightarrow C$ : Assume B. Since  $B \Leftrightarrow A$ , A is true.

Therefore,  $v_b$  lies strictly in region I of  $v_a$ . Hence, there exists a small region, say a circle of radius  $\epsilon$  (a small length) around  $v_b$ , which also lies completely in region I (figure 5).

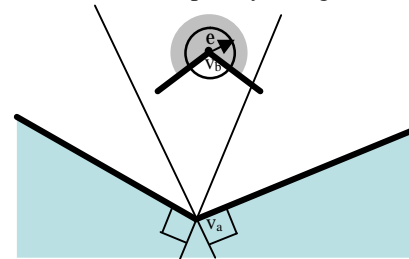


Fig. 5.  $\sigma(v_a, s_b)$  is a local maximum of  $\sigma(s_a, s_b)$  for any  $s_b$  in the neighborhood of  $v_b$ .

Consider any  $v'_a$  in  $P$ , within  $\epsilon$  from  $v_a$ , and  $v'_b$  in  $P$  within  $\epsilon$  from  $v_b$ . Since  $v_a$  is in  $v_b$ 's region I,  $\sigma(v_a, s_b)$  is a local maximum at  $s_b = v_b$ . Therefore,  $v_a v_b > v_a v'_b$ . Since  $v'_b$  also lies in  $v_a$ 's region I,  $v_a v'_b > v'_a v'_b$ . Thus,  $v_a v_b > v'_a v'_b$ . Therefore,  $C \Leftrightarrow B$ .

$C \Rightarrow D$ : Assume C is true and D is false. Since  $A \Leftrightarrow C$ , A is true. Since  $\sigma(v_a, v_b)$  is a local maximum and D is false, the part is not in form-closure. This means that there exists a neighboring point in C-space that does not result in collision. In other words, the part can be displaced infinitesimally. Since C is true, at least one jaw must break contact with the part in the new configuration.

If both jaws break contact, we can move the part along the directions  $\pm \mathbf{u}_{ab}$  till contact occurs as both vertices are concave and hence have an angle of less than  $180^\circ$  from the direction of the jaws' approach. As a result, movement in at least one of two opposite directions results in contact. From this position, we can slide the part along the contact edge moving the vertex towards the jaw, till contact occurs with the other jaw or till the vertex is at the jaw. Since  $v_a v_b$  is a strict maximum, the vertex has to be reached. However, since A is true,  $\mathbf{u}_{ab}$  is at acute angles to  $\mathbf{u}_{a-1}$  and  $\mathbf{u}_{a+1}$ , and  $\mathbf{u}_{ba}$  is at acute angles to  $\mathbf{u}_{b-1}$  and  $\mathbf{u}_{b+1}$ . Therefore, when the vertex reaches the jaw, the other jaw would collide with the interior of the part: thus the part cannot move and is in form-closure.

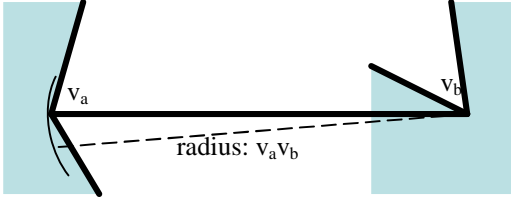


Fig. 6. The edges are at acute angles to  $v_a v_b$ .

$D \Rightarrow C$ : Assume D is true and C is false. Then,  $\sigma(v_a, v_b)$  is not a local maximum. Either it is a strict local minimum or it is not a strict local extremum. If  $v_a v_b$  is a strict local minimum it can be shown that  $\langle v_a, v_b \rangle$  is a contracting v-grip, and hence D cannot be true. If  $v_a v_b$  is not a strict extremum, then by the continuity of  $s$ , the part can move along the contour  $\{(s_1, s_2) \mid \sigma(s_1, s_2) = \sigma(v_a, v_b)\}$ . This contradicts D. Therefore C is true.

Thus,  $D \Leftrightarrow C$ , completing the proof for theorem 1. We can prove Theorem 2 similarly. The second condition in Theorem 2 arises due to the limiting case where vertex lies on the boundary of region IV.

**Corollary 1:** If the second condition in theorem 2 is ignored, and all the inequalities are made strict inequalities in theorem 2, theorems 1 and 2 give necessary and sufficient conditions for first order immobility.

This can be proved from 1) first order form-closure is a subset of immobility, and 2) center of rotation analysis. For the center of rotation analysis, all the configurations excluded by making the conditions in theorem 2 stricter can be seen to be second order immobility as they give rise to coincident normals that cannot cause first order immobility, but cause immobility. Also, the remaining configurations are first order because the normals cannot coincide and cannot be concurrent (as 2 of the 4 points of intersection are at distinct vertices), and all centers of rotation are excluded as we know the part is immobile.

**Corollary 2:** For a non-point jaw with a convex shape, the v-grips can be generated by applying the theorems to a transformed part generated by doing a Minkowski sum of the part's shape with the jaws' shape.

This can be seen as the transformed part gives the locations of the jaws' center that result in collision with the part, and thus also the shape of the cross sections of the C-obstacles. The curved edges generated by doing the sum can be ignored as they correspond to contact with convex vertices, which we seek to avoid.

#### D. 2D Quality Metric

We can compare v-grips based on how much the part can rotate when the jaws are relaxed infinitesimally. We define a measure of the sensitivity of the grip to such infinitesimal disturbances. Given a v-grip  $\langle v_a, v_b \rangle$ , let  $l = \sigma(v_a, v_b)$ . If the distance between the jaws changes by  $\Delta l$ , let  $\Delta \phi$  be the maximum angle the part can rotate. Clearly,  $\Delta \phi$  depends on  $\Delta l$ . We consider the ratio  $\Delta \phi / \Delta l$ , which for infinitesimal changes becomes  $d\phi / dl$ . We rank parts based on  $|d\phi / dl|$ : smaller ratios correspond to more robust grips. It can be shown that the maximum  $|d\phi / dl|$  occurs when both jaws are in contact with the part with one of them at a vertex.

To derive an expression for  $|d\phi / dl|$ , we consider one edge at an angle  $\phi$  to  $v_a v_b$ . Using the sine rule,

$$(l - \Delta l) / (\sin \mathbf{f}) = l / (\sin(\phi + \Delta \phi))$$

If we neglect second order terms, this simplifies to:

$$|d\mathbf{f} / dl| = \lim_{\Delta l \rightarrow 0} |\Delta \mathbf{f} / \Delta l| = |\tan(\mathbf{f}) / l|$$

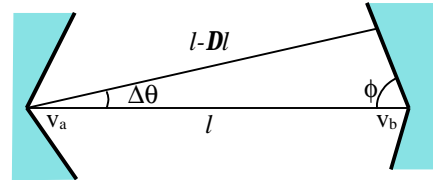


Fig. 7. Deriving an expression for  $|d\phi / dl|$ .

For all 4 edges, we choose the one with  $\phi$  closest to  $90^\circ$ , which yields the maximum possible change in orientation. For this value of  $\phi$ , the metric will be  $|\tan(\phi) / l|$ . We use this metric to rank v-grips.

### V. KINEMATIC ANALYSIS: 3D VG-GRIPS

#### A. Problem Definition

In the first phase of our two-phase design procedure, we assume the part is rigid and proceed to design and determine the locations of 2 jaws to fixture the 3D sheet metal part. We will make use of the results on fixturing 2D parts for this.

The primary jaws are designed to engage the part at its concavities such that the intersections of the frustums in the jaws are seated in the plane of the sheet metal part. For the part to contact the jaws on the plane of intersection of its frustums, the local radius of curvature of the part needs to be large compared to the jaws' radius. If this is not true, contact does not occur on the plane, but instead, on the surfaces of the individual cones. Therefore, at such candidate jaw locations, we assume local planarity of the part and linearity of the edges for first order analysis of immobility, since only local shape is of importance. We construct tangents at the points of contact. We call these tangents the part's "virtual edges", and the point of intersection of the edges, the corresponding "virtual vertex". If we approximate the part locally using the virtual edges and vertices, immobility of the approximation will be equivalent to the immobility of the original part up to the first order. The jaws' positions are described in terms of the virtual vertices. Virtual vertices are concave by definition. Given 2 virtual vertices  $v_a$  and  $v_b$ , we call the unordered pair  $\langle v_a, v_b \rangle$  a vg-grip

if the part is held in form-closure when the jaws' grooves engage the part at the edges defining  $v_a$  and  $v_b$ .

The FEM portion of the input such as the mesh and the part's material properties are irrelevant for this phase. This phase can give an output of a list (possibly empty) of vg-grips for the part, with bounds on jaw cone angles for each listed vg-grip, sorted by the quality metric described below.

### B. Candidate Jaw Locations

As stated above, while contact occurs near vertices for a part defined by linear edges, parts with curved edges have virtual vertices near which the jaws engage the part. Each virtual vertex corresponds to a unique candidate jaw location where a jaw may be located to engaging the part at the virtual edges corresponding to the vertex. Candidate jaw locations and corresponding virtual vertices are identified using the algorithm described below.

The algorithm uses the fact that jaws contact the part at 2 points only if there is a concave vertex between the points of contact or if part of the edge contained between the points of contact is concave and has higher curvature than the jaw.

Step 1: Set list  $L$  as list of the part's concave vertices. Set list  $L_c$  to an empty list.

Step 2: Traverse each edge of the part. For each edge, numerically identify concave stretches with radius of curvature less than jaw radius, and add the end points (with higher arc-length) to  $L$ .

Step 3: For each point  $i$  in  $L$ , traverse the edge starting from the point  $i$  in the direction of increasing arc-length, constructing discs tangential the edge till the disc touches the part at 2 points or the entire edge is traversed back up to the position of the current element of  $L$ .

If the entire edge was not traversed and if the edge at the second point of contact is in plane with the disc, add the center to  $L_c$ . Replace the current element of  $L$  by the point of intersection of the tangents.

Else, delete the current element of  $L$ .

Step 4: Traverse  $L_c$  for duplicates and eliminate them and the corresponding elements in  $L$ .

Step 5: Return the list  $l$  as the list of candidate locations and  $L_c$  as the list of centers.

### C. Sufficient Test

As shown in Figure 8, we define a coordinate system such that the direction of the  $x$  axis is taken from  $v_a$  to  $v_b$ . In a projection perpendicular to the  $x$  axis, the  $z$  axis is defined as the bisector of the acute angle between the projections of jaw axes. When jaw axes projections are parallel, the  $z$  axis is defined at  $45^\circ$  to the jaws' axes. The  $y$  axis is perpendicular to the  $x$  and  $z$  axes using the right hand rule. Let the points of contact have position vectors  $\mathbf{r}_{a1}$ ,  $\mathbf{r}_{a2}$ ,  $\mathbf{r}_{b1}$  and  $\mathbf{r}_{b2}$ . Let the vectors  $\mathbf{a}_a$  and  $\mathbf{a}_b$  be the axes of the jaws with positive  $z$  components and the centers of the intersections of the cones be  $c_a$  and  $c_b$ . (The subscripts  $a$  and  $b$  denote the jaws at vertices  $v_a$

and  $v_b$ .) We define  $\mathbf{q}_{a1}$  as:  $\mathbf{e}_x \times ((\mathbf{r}_{a1} - \mathbf{v}_a) - (\mathbf{r}_{a1} - \mathbf{v}_a \cdot \mathbf{e}_x) \mathbf{e}_x) = \mathbf{e}_x \times (\mathbf{r}_{a1} - \mathbf{v}_a)$ , and similarly  $\mathbf{q}_{b1}$ ,  $\mathbf{q}_{a2}$  and  $\mathbf{q}_{b2}$ .

**Theorem 3:** Assuming that the part is rigid, immobility is achieved if all of the following are satisfied:

- The projection of the part and jaws on the  $x$ - $y$  plane is an expanding 2D v-grip.
- The projection of the part and jaws on the  $x$ - $z$  plane is an expanding 2D v-grip.
- The angle between  $\mathbf{q}_{a1}$  and the inward normal to at least one of the cones at  $\mathbf{r}_{a1}$  is less than  $90^\circ$ , and the angle between  $-\mathbf{q}_{a1}$  and at least one of the inward normals at  $\mathbf{r}_{a1}$  is less than  $90^\circ$ . And similarly for  $\mathbf{q}_{a2}$ ,  $\mathbf{q}_{b1}$ ,  $\mathbf{q}_{b2}$ .

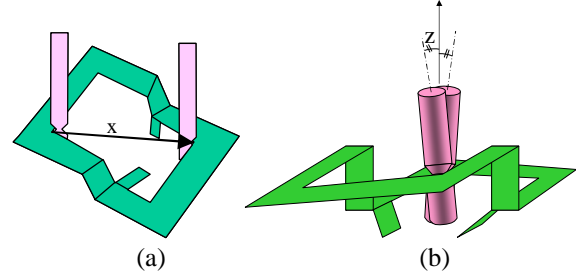


Fig. 8. (a) The  $x$  axis is chosen along the line connecting the vertices  $v_a$  and  $v_b$ . (b) In a projection perpendicular to the  $x$  axis, the  $z$  axis is chosen as the bisector of the acute angle between the jaws' axes' projections.

### D. Proof of Theorem 3

The distance between the jaws is defined as the  $x$  component of the distance between the centers of the cones' intersections. We will show that any small displacement of the part requires a decrease in distance between the jaws if one jaw is fixed and the other is allowed to translate. Hence, since the jaws are fixed, the part will be in form-closure.

Consider any small displacement of the part. This can be denoted as the sum of 3 translations and 3 rotations (along and about the  $x$ ,  $y$  and  $z$  axes). We show that as the part is subject to each of these components of displacement while keeping the distance between them at the local maximum of the possible distances, the distance between them decreases.

From condition (c) in Theorem 3, any rotation of the part about the  $x$  axis should result in a decrease of distance between the jaws. This is because the vectors  $\mathbf{q}_{xi}$ ,  $x=a, b; i=1, 2$ , give the direction of the instantaneous velocities of each contact. Hence, if a jaw stays in the same position, it collides with the part, i.e. it has to move either towards or away from the vertex. It cannot move towards the vertex because of the following reason: if we scale down the part and the jaw about the vertex, such that the distance between the scaled jaw and the vertex is equal to the distance between the vertex and the jaw after the rotation, the scaled jaw would collide with the part after an identical rotation (since the conditions are scale-independent). Since a smaller jaw would collide with the part in such a position, the original bigger jaw will also collide with the part, since the vertex and edges of the part do not change on scaling. Hence, each jaw is pushed away from the vertex.

First order form-closure is robust in the sense that immobility is guaranteed allowing for small changes in part

geometry. Since none of the axes are perpendicular to the planes of intersections of each jaw's cones, conditions (a) and (b) of Theorem 3 ensure that the projections of the part on the x-y and x-z planes are in form-closure after an infinitesimal rotation of the part about the x axis. We note that the distance between the vertices does not change as a result of rotation about the x axis. Since the distance between the vertices remains the same due to such a rotation and since the edges are linear and the vertices concave, it follows from Theorem 1 that the distance between the jaws decreases.

Condition (a) also implies that translation along the x or y axes, and rotation about the z axis will result in further increase in the distance between the jaws. Condition (b) implies that any further translation along x or z axes and rotation about the y axis leads to another increase in distance. Thus, any displacement of the part results in a displacement of the jaws, hence proving that form-closure is achieved if the jaws are fixed.

### E. Bounds on Cone Angles

Conditions (a) and (b) in theorem 3 are independent of the cone shapes for a given jaw radius. Hence, bounds on the cone angles that satisfy Theorem 3 are determined only by the condition (c). In the worst case,  $\pm \mathbf{q}_{xi}$ ,  $x=a, b$ , are tangential to the cones for at least 1 value of  $i=1, 2$ . Hence, if we project  $\pm \mathbf{q}_{xi}$  to the plane containing  $\mathbf{r}_{xi}$  and  $\mathbf{a}_x$ , the acute angles between the projections and  $\pm \mathbf{a}_x$  give a candidate lower bound for the half cone angle for the upper cone. For instance, the lower bound is chosen as the higher of candidate bounds obtained from  $\mathbf{q}_{x1}$  and  $\mathbf{q}_{x2}$ . For the 3D sheet metal part example shown in figure 1, the bounds for the half cone angles for the 4 cones were  $18^\circ, 21^\circ, 18^\circ$ , and  $26^\circ$ .

### F. 3D Quality Metric

We propose as an intuitive fixture quality metric the maximum change in orientation along any of the coordinate axes due to an infinitesimal relaxation of the jaws. This is based on the metric described in section IV for 2D v-grips. It is quantified by  $|d\mathbf{q}/dl|$ ,  $l$  being the distance between the jaws, and  $\mathbf{q}$  the orientation. For the y and z components, this reduces to the metric obtained from the 2D v-grip metrics. For rotation about the x axis, this is not the case. We find an approximate value for  $|d\mathbf{q}/dl|$  by assuming that the contacts lie on the vertices of the v-groove in the projection of the jaws on a plane perpendicular the plane containing the contacts and the edges. Since the contacts on the jaw projection hold the jaw in a v-grip, we know that distance between the contacts increases by  $q_a D\mathbf{q}$ , where  $q_a$  is the quality metric for this v-grip. Hence, if the original distance between the centers of jaw  $a$  and the vertex is  $d_a$ , the distance after rotation is  $d_a(1 + q_a D\mathbf{q}/|\mathbf{r}_{a1} - \mathbf{r}_{a2}|)$ . Thus, the metric for rotation about the x axis simplifies to  $(|\mathbf{r}_{a1} - \mathbf{r}_{a2}|/d_a q_a + |\mathbf{r}_{b1} - \mathbf{r}_{b2}|/d_b q_b)$ . The quality of the v-grip is the maximum of the metrics for all 3 rotations.

## VI. PART DEFORMATION

Once the first phase is completed, we get a list of pairs of jaws that can fixture the rigid sheet metal part. For each of

these, we introduce a deformation model that is the second phase of our analysis. We use the deformation model to add more jaws (if necessary) to reduce deformations to within the tolerance using the algorithm described in section VII.

To model part deformation we use FEM, based on the given FEM mesh. We have used quadrilateral elements in our implementation, but this can be generalized to other meshes too. Rigid jaws constrain the positions of the nodes on which they lie. By the nature of the expanding v-grip, the forces exerted by each jaw on the part are directed away from each other. All jaws added in the second phase will also not create compressive forces that cause buckling. Also, since any jaw that is added to the fixture can constrain the part only if the jaw does not lose contact with the part as it deforms, all new jaws are conical jaws placed at part edges or surface support jaws away from the edges where deflection is towards the sheet metal part's interior direction on which the unilateral fixture lies.

## VII. ALGORITHM

Based on sections IV through VI, we describe below our two-phase unilateral fixture design algorithm for sheet metal parts:

### (Phase I: Kinematic analysis)

Step 1: Set list of fixtures  $L_f$  to be empty.

Step 2: Generate a list of all virtual vertices. Store this as  $(v_1, v_2, v_3, \dots)$

Step 3: For each unordered pair of vertices  $\langle v_i, v_j \rangle$ , apply Theorem 1 to determine if  $\langle v_i, v_j \rangle$  is a v-grip.

### (Phase II: Deformation model)

Step 4: For each v-grip  $\langle v_i, v_j \rangle$ , with primary jaws at  $v_i$  and  $v_j$ :

- i. Define  $E$  = the set of candidate edge nodes and  $F$  = set of candidate face nodes as all mesh nodes of the part's perimeter and interior respectively.
- ii. Traverse  $E$  and remove nodes  $j$  if either:
  - a. Jaw at  $j$  and primary jaws collide, or
  - b. Jaw at  $j$  and any primary jaw cause the part to buckle (the pair exerts a compressive force).
- iii. With the current set of jaws, compute the deformation of the part at each node.
- iv. Determine the maximum deformation  $d$ .
- v. If this  $d < \delta$ , add the current fixture to  $L_f$  and go to step 5.
- vi. If  $E$  and  $F$  are empty, proceed to next v-grip from step i.
- vii. Let maximum deformation for all jaws in  $E$  and  $F$  occurs at node  $i$ . If  $i$  is an edge node, place a conical jaw at the candidate node. Else, if the deformation at  $i$  is towards the interior of the assembly, place a point contact at  $i$ . with maximum deformation normal to the part (call it node  $i$ ).
- viii. If  $i$  is in  $E$ , then from  $E$  remove node  $i$  and all nodes  $j$  such that either:
  - a. Jaws at  $i$  and  $j$  collide, or

b. Jaws at  $i$  and  $j$  cause the part to buckle (they exert a compressive force).

Else, remove  $i$  from  $F$ .

ix. Go to step iv.

Step 5: For each fixture, compute bounds on cone angles and store them in  $L_f$ .

Step 6: Return  $L_f$ , the list of acceptable fixtures and bounds on cone angles.

The algorithm generates a natural actuation order. However, this need not be the best order in which to actuate each jaw.

### VIII. COMPLEXITY AND IMPLEMENTATION

Recall that the polygonal part is described by  $n$  vertices. For the polygonal part, we find  $k \leq n$  concave vertices flanked by straight edges in  $O(n)$  time. We then consider each pair of concave vertices, checking the conditions in Theorems 1 and 2 in constant time. The result is a set of up to  $k^2$  v-grips. Thus, all v-grips are found in  $O(n + k^2)$  time. Computing the quality metric takes constant time for each v-grip and sorting requires  $O(k^2 \log k)$  time as there are at most  $k^2$  v-grips. We implemented the algorithm in Visual BASIC.

On a Pentium II 266 MHz PC running on Windows NT 4.0, the program execution time was under 0.02 seconds for a part with 30 vertices and 10 concave vertices, while interpreting. A Java implementation is available for online testing at <http://alpha.ieor.berkeley.edu/vgrip>.

For a sheet metal part, given  $n$  virtual vertices, there are at most  $O(n^2)$  pairs of candidate jaw locations. For each pair, the algorithm is applied in constant time. Hence phase I runs in  $O(n^2)$  time.

In phase II, if the FEM mesh has  $m$  nodes, at most  $m$  secondary jaws are needed as deformations are at maxima at the mesh nodes. Hence, for  $r$  jaws, the algorithm runs in  $O(m^3 r)$  time for each vg-grip.

Figure 9 shows an example of the first 2 iterations (figures 9(a) and 9(b)) for an example part. For a tolerance of 1mm, the fixture is shown in figure 9(c). All 4 FEM iterations together required 1.3 seconds. More examples are shown in figure 9(d).

### IX. EXPERIMENTS

To test the precision in orientation of parts loaded on the fixtures, we consider two physical parts: a glue gun held by 2 jaws and an automotive part held by 3 jaws. We built 2 fixtures to hold these parts and conducted repeated trials and observed the orientation of the loaded part. Since the jaws engage the part at precise features of the part, the orientation is more significant than the position in terms of contribution to errors in the positions of datum points.

#### A. Glue gun

The first set of experiments was for a plastic, one foot long, glue gun part held by 2 jaws with radii 0.5 inches each. The jaws moved at a speed of 0.01 inches/second. The part was mounted on a set of bearings on a Plexiglas surface. Three calibrated video cameras and a laser beam mounted on the part were used to record the positions and orientations of the part

for the fixtures shown in Figure 10(a) and (b), before and after the grip. The jaws moved at a speed of 0.1 inches/second. One hundred trials at random initial orientations were carried out for each fixture.

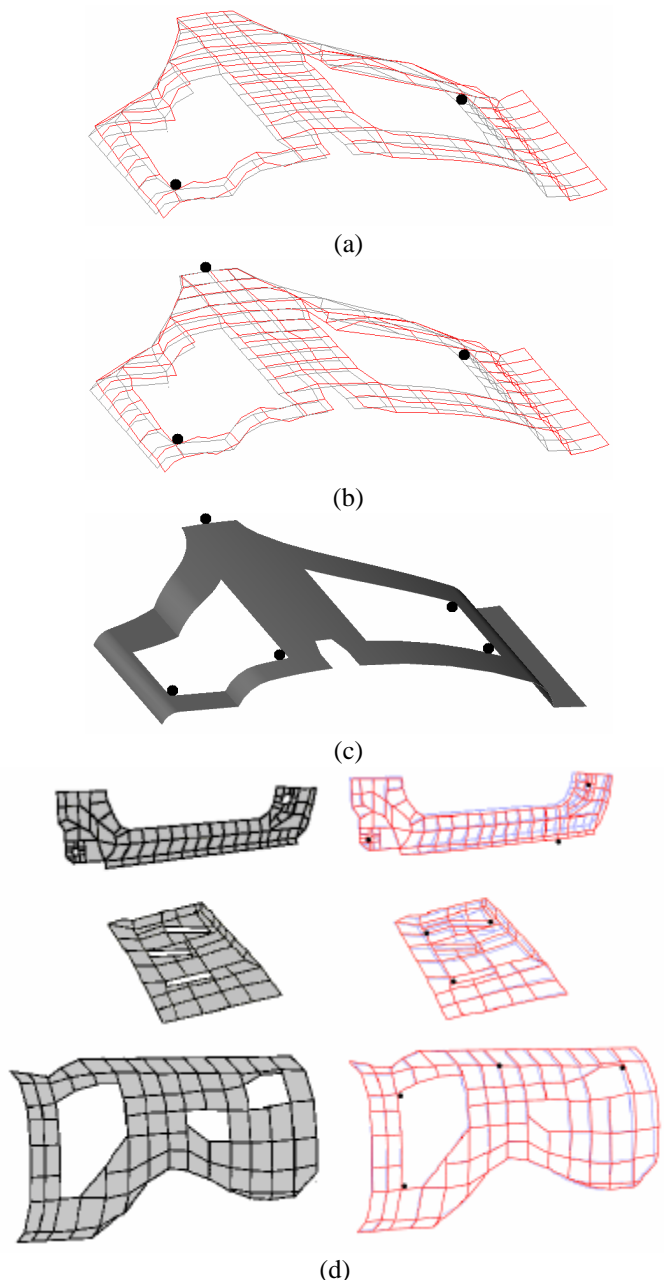


Fig. 9. Deformed and undeformed meshes for first 2 iterations of Phase II. Final fixture (c) required 4 iterations. More example parts and the corresponding jaw locations and meshes are shown in (d).

Figure 10(c) is a photograph of the apparatus used to test the v-grips and figure 10(d) shows a histogram of the orientation error distributions for the 2 v-grips. For the first, the error ranged from -0.22 to +0.09 degrees. The mean error magnitude was 0.083 degrees and the standard deviation was 0.083 degrees too. For the second v-grip, the error ranged from -0.20 to +0.09 degrees. The mean magnitude and the standard deviation were 0.08 and 0.07 degrees respectively.



There was a high correlation between the signs (positive/negative) of starting and ending orientations for the first v-grip, and a lesser correlation for the second.

The main sources of error identified are the friction between the part and the jaws and the rounded edges of the part (non-prismatic part) that result in the jaws lifting the part off the plane.

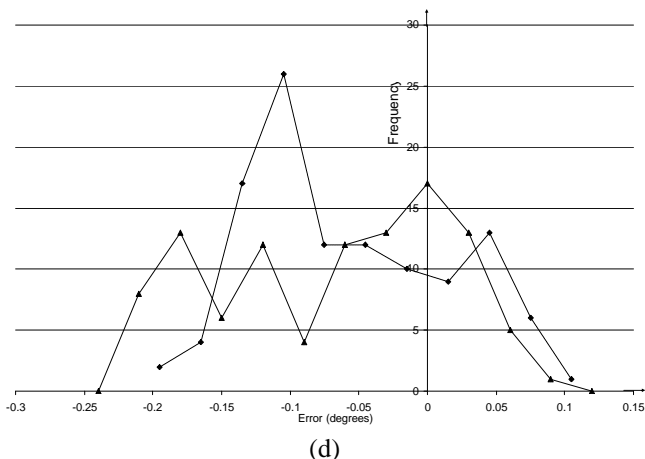
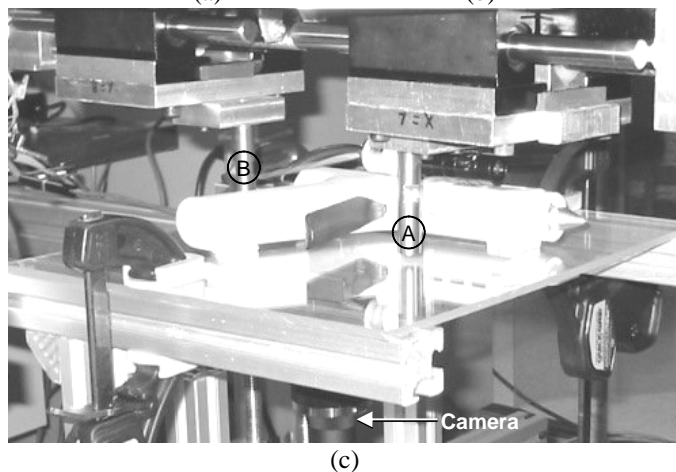
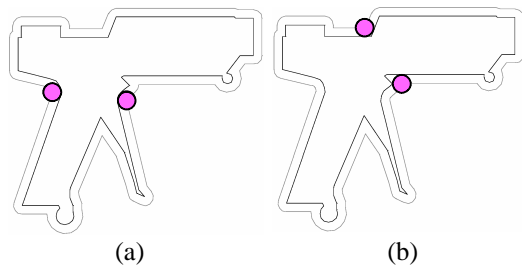


Fig. 10. Using the apparatus shown in (c), trials with v-grips (a) and (b) yielded the error distributions for shown in (d) with sampling intervals of  $0.03^\circ$ . The continuous line corresponds to grip (a) and the broken line is grip (b).

### B. Unilateral Fixtures

We constructed a prototype of a unilateral fixture for an automotive part. The prototype consisted of two parts: the loading jig and the fixture. The loading jig consists of supports on which the part can be placed prior to actuation of the fixture's jaws. Once the fixture's jaws are actuated to grip the part and the part is acquired, the fixture is separated from the loading jig.

The prototype was constructed for an automotive part made of chrome-plated steel and about 8" long. The prototype makes use of 2 Plexiglas base-plates, one each for the loading jig and the fixture. The loading jig consisted of 3 point-contacts and the fixture consisted of one fixed jaw and 2 jaws actuated by solenoids. The jaws move along dovetail tracks when actuated. The base-plate of the fixture can be mounted on top of the base-plate for the loading jig and can be lifted off after the jaws are actuated. To measure the orientation of the part, a laser beam is reflected off a mirror mounted on the part and position of the reflected beam on a reflected beam is recorded. In order to minimize the sensitivity of the observations to the part's positions and maximize sensitivity to orientations, the part and the surface where the beam is observed need to be made as close to perpendicular to the reflected beam as possible.

Fifty trials each were carried out with the prototype for simultaneous actuations of the movable jaws and both sequences of actuation of the jaws one at a time. Error in orientation was determined using laser beams reflected by the part. Figure 11(a) and (b) show the prototype and figure 11(c) shows the resulting histograms of the orientation error.

Actuating the jaw A in figure 11 before jaw B resulted in higher precision. However, the actuation force required was much more than that when both were actuated simultaneously. Also, the initial range of allowable orientations (or capture region) was higher for simultaneous actuation. 3 outliers for actuating jaw B first and 2 for actuating jaw A first have been eliminated from the histogram since the part was not within the capture region resulting in the part not being acquired properly.

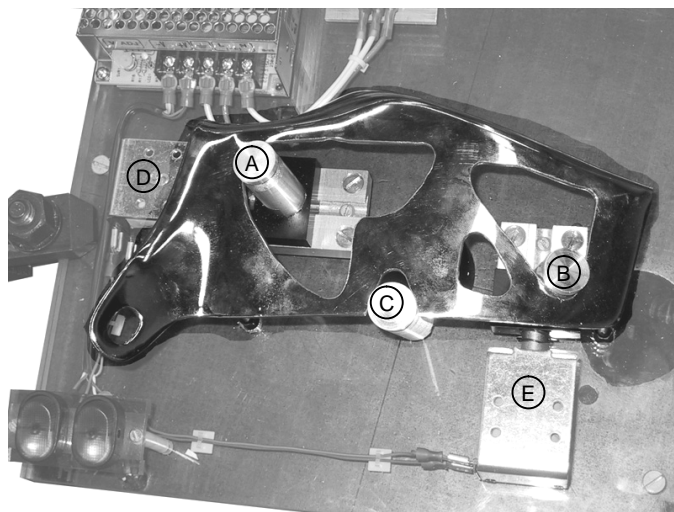
## X. EXTENSIONS AND FUTURE WORK

Future work will consist of finding a locator strategy for mating parts during welding. Sheet metal parts need to be positioned with appropriate gaps for the welding process and the deformation due to warping after welding needs to be minimized. We will also look into using multiple primary locators so as to not restrict jaw locations too much. We will also consider other types of modular jaws. In parallel, we will also look at other aspects of design like designing the part for manufacturability, especially in terms of placing precise locator holes in the part that aid in fixturing it.

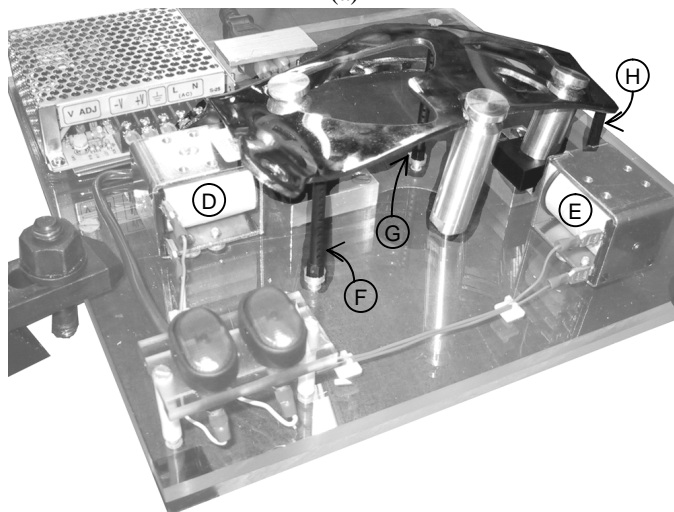
We are also looking into using the fixture as a curing fixture to bond two sheet metal parts using adhesives along the perimeter. This requires control of the gap between the fixtures. We are also working on algorithms for designing loading jigs for the fixtures.

### ACKNOWLEDGMENT

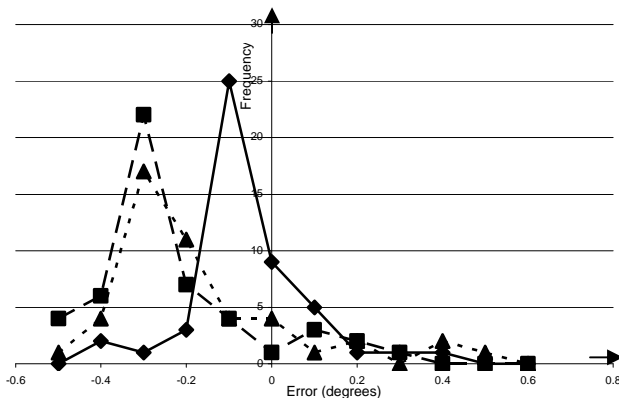
The authors thank Josh Alton, Ron Alterovitz, Anthony Levandowski, Dezhen Song and Paul Wright for their contribution and feedback.



(a)



(b)



(c)

Fig. 11. Unilateral fixture prototype shown in (a) and (b) has 2 CE contacts A and B actuated by solenoids D and E. C is a SE contact. F, G and H are LS contacts. Trials with the prototype yielded the error distributions for shown in (c) with sampling intervals of  $0.1^\circ$ . The jaws at the left and at the right are the CE contacts. The continuous line corresponds to simultaneous actuation, the dashed line corresponds to actuating the right jaw first, and the dotted line corresponds to activating the right jaw first.

## REFERENCES

- [1] A. Blake and M. Taylor, Planning Planar Grasps of Smooth Contours, IEEE International Conference on Robotics and Automation, vol. 2, pp 834-839, 1993.
- [2] A. Bicchi and Vijay Kumar, Robotic Grasping and Contact: A Review, Proceedings of IEEE International Conference on Robotics and Automation, pp348-353, 2000.
- [3] Randy C. Brost and Kenneth Y. Goldberg. A complete algorithm for designing planar fixtures using modular components. IEEE Transactions on Robotics and Automation, 12(1); 31-46, February 1996.
- [4] Cai W., Hu S.J., Yuan J.X., Deformable sheet metal fixturing: principles, algorithms, and simulations. Transactions of the ASME. Journal of Manufacturing Science and Engineering, vol.118, (no.3), ASME, Aug. 1996. p.318-24.
- [5] J. F. Canny, K. Y. Goldberg, "RISC" industrial robotics: recent results and open problems, IEEE International Conference on Robotics and Automation, vol.3, pp.: 1951 -1958, 1994.
- [6] Dan Ding, Guoliang Xiang, Yun-Hui Liu, Wang M Yu, Fixture layout design for curved workpieces, Proceedings, IEEE International Conference on Robotics and Automation, 2002, Volume: 3, Page(s): 2906 -2911 vol.3, 2002.
- [7] [http://toyota.irweb.jp/IRweb/corp\\_info/body\\_line/](http://toyota.irweb.jp/IRweb/corp_info/body_line/) Global Portal, Toyota.
- [8] K. "Gopal" Gopalakrishnan, Ken Goldberg, Gripping parts at concave vertices, IEEE International Conference on Robotics and Automation, 2002, Page(s): 1590 -1596, Volume: 2 , 2002.
- [9] Hurtado J.F., Melkote S.N., Effect of fixture design variables on fixture-workpiece conformability and static stability, Proceedings, 2001 IEEE/ASME International Conference on Advanced Intelligent Mechatronics, Volume: 1, Page(s): 189 -194 vol.1, 2001.
- [10] Li B., Shiu B.W., Lau K.J., Fixture configuration design for sheet metal assembly with laser welding: a case study. International Journal of Advanced Manufacturing Technology, vol.19, (no.7), Springer-Verlag, 2002. p.501-9.
- [11] X. Markenscoff, L. Ni and C. H. Papadimitriou, The Geometry of Grasping, International Journal of Robotics Research, Vol. 9, No. 1, pp 61-74, 1990.
- [12] Mason M.T., Mechanics of Robotic Manipulation, The MIT Press, 2001.
- [13] Menassa R., De Vries W., Optimization Methods Applied to Selecting Support Positions in Fixture Design, ASME Journal of Engineering for Industry, vol 113, pp. 412-418, 1991.
- [14] B. Mishra, J. Schwarz, and M. Sharir, On the existence and Synthesis of Multifinger Positive Grips, Algorithmica 2, 1987.
- [15] Plut, W.J., Bone, G.M., Limited mobility grasps for fixtureless assembly, Robotics and Automation, 1996. Proceedings., 1996 IEEE International Conference on , Volume: 2 , 1996, Page(s): 1465 -1470 vol.2.
- [16] Plut, W.J., Bone, G.M., 3-D flexible fixturing using a multi-degree of freedom gripper for robotic fixtureless assembly, Robotics and Automation, 1997. Proceedings., 1997 IEEE International Conference on , Volume: 1 , 1997, Page(s): 379 -384 vol.1.
- [17] Jean Ponce, Joel Burdick and Elon Rimon, Computing the Immobilizing Three-Finger Grasps of Planar Objects, Proceedings of the Workshop on Computational Kinematics, 1995.
- [18] Rearick M.R., Hu S.J., Wu S.M., Optimal Fixture Design for Deformable Sheet Metal Workpieces, Transactions of NAMRI/SME, vol. XXI, pp. 407-412.
- [19] F. Reuleaux, The Kinematics of Machinery. New York: Macmillan 1876, republished by New York: Dover, 1963.
- [20] Rimon E. and Burdick J., On force and form closure for multiple finger grasps, Proceedings of IEEE International Conference on Robotics and Automation, 1996, pp. 1795 -1800 vol.2.
- [21] Elon Rimon and Joel Burdick, Mobility of bodies in contact - I, IEEE transactions on Robotics and Automation, 14(5): 696-708, 1998.
- [22] Rimon, E. and Blake, A., Caging planar bodies by one-parameter two fingered gripping systems, International Journal of Robotics Research, v18, n3, March 1999, pp. 299-318.
- [23] Rong, Y., Li, X.-S., Locating method analysis based rapid fixture configuration design, Proceedings, 6th International Conference on Emerging Technologies and Factory Automation ETFA '97, Page(s): 27 - 32, 1997.

- [24] Salisbury, J.K. Kinematics and Force Analysis of Articulated Hands. Ph.D. Thesis, Stanford University, 1982
- [25] Sela M.N., Gaudry O., Dombre E., Benhabib B., A reconfigurable modular fixturing system for thin-walled flexible objects, International Journal of Advanced Manufacturing Technology, 13:611-617, 1997.
- [26] P. Somoff, Über gebiete von schraubengeschwindigkeiten eines starren körpers bievverschiedener zahl von stuz achen, Zeitschrift für Mathematic and Physik, vol. 45, pp. 245-306, 1900.
- [27] Van der Stappen A.F., Wentink C., Overmars M.H., Computing form-closure configurations, Proceedings of IEEE International Conference on Robotics and Automation, vol.3, pp. 1837 -1842, 1999.
- [28] Michael Yu Wang, Pelinescu D.M., Optimizing fixture layout in a point-set domain, IEEE Transactions on Robotics and Automation, Volume: 17 Issue: 3 , Page(s): 312 -323, June 2001.
- [29] M. Y. Wang, Tolerance analysis for fixture layout design, Assembly Automation, a special issue on Automated Fixturing, vol. 2, no. 2, pp. 153 – 162, 2002.
- [30] Wang M.Y., Tong Liu, A full contact model for fixture kinematic analysis, IEEE/RSJ International Conference on Intelligent Robots and System, 2002, Volume: 2, Page(s): 1602 -1607, 2002.
- [31] Xiong C., Rong Y., Koganti, R.P., Zaluzec M.J., Wang N., Geometric variation prediction in automotive assembling, Assembly Automation, vol. 22, No. 3, pp. 260-169, 2002.